

Superradiant State of Josephson Plasma and Moving Josephson Vortices in Copper Oxide Superconductors

Masashi Tachiki

National Research Institute for Metals, Sengen 1-2-1, Tsukuba, Ibaraki, 305-0047, Japan Fax:81-298-59-2407,
email:tachiki@nrim.go.jp

Masahiko Machida

Argonne National Laboratory, MSD223, 9700 S. Cass Ave. Argonne, IL 60439, US
and

Japan Atomic Energy Research Institute, 2-2-54 Nakameguro, Meguro-ku, Tokyo 153-0061, Japan *

Natural arrays of Josephson junctions are constructed in High-Tc cuprate superconductors like $\text{Bi}_2\text{Sr}_2\text{CaCu}_2\text{O}_{8+y}$. In the junction arrays a unique excitation called Josephson plasma occurs. By applying an external magnetic field parallel to the CuO_2 plane, the Josephson vortices are introduced into the sample. When an external current flowing along the c -axis drives vortices, they move very fast along the ab -plane, since the Josephson vortex has not a normal core in contrast to the usual Abrikosov vortex. In certain values of external current and magnetic field, the moving Josephson vortices resonate the Josephson plasma waves, leading to some transformations between different vortex lattice configurations and radiations of electrodynamical wave. Especially, when a rectangular vortex lattice aligned along the c -axis appears, a superradiant state of electromagnetic wave can be expected to appear. This phenomenon is quite useful for an electromagnetic wave generation in Tera-Hertz high frequency range.

Key Words: oxides, High-Tc superconductors, Josephson plasma, superradiant state, submillimeter wave generation

I. INTRODUCTION

Cuprate High-Tc superconductors are layered materials composed of CuO_2 superconducting layers and other block layers. Therefore, some materials among them show strong anisotropy for the electron conduction along the a - b plane and the c -axis direction. A typical example of High-Tc materials exhibiting such strong anisotropy is $\text{Bi}_2\text{Sr}_2\text{CaCu}_2\text{O}_{8+y}$ (Bi-2212). In Bi-2212, the block layers work as insulating layers and the neighboring double CuO_2 layers are coupled by the Josephson effect. Thus, Bi-2212 constructs a natural array of Josephson junctions and is called an intrinsic Josephson junction. In fact, Kleiner et al. [1] and Oya et al. [2] independently observed Josephson effects themselves in the single crystals of Bi-2212. In the intrinsic junction systems, there is a question whether all the junctions can synchronize each other in their oscillating states. If it is accessible in a wide frequency range, it means that the system is quite useful as an electronic oscillators. Therefore, the synchronization is the important issue when the intrinsic Josephson junctions are considered for electromagnetic devices. In this paper we discuss the synchronization phenomena under an external magnetic field applied parallel to the a - b plane and the transport current applied parallel to the c -axis. In the intrinsic Josephson junction, there exist two types of excitations in terms of dynamics of the super-

conducting phase. The first one is the Josephson plasma mode which is an oscillating wave propagating inside the sample [3] and the second one is the Josephson vortex [4]. Theoretically both of the first and the second excitations can be described as linear and non-linear solutions in the basic equation describing the dynamics of the phase difference between neighboring superconducting layers, respectively. In a single Josephson junction system in which the Sine-Gordon equation is a good description in studying the dynamics of the phase difference, the Josephson plasma mode corresponds to a plane wave solution of the linearized Sine-Gordon equation, while the Josephson vortex is given by a soliton solution in the Sine-Gordon equation [5]. In the intrinsic Josephson junction, both the excitations are expected to be more complicated. For example, the Josephson plasma wave can propagate even along the junction stacking direction [6], that is, the c -axis, in addition to the junction a - b plane, while the Josephson vortices form a two dimensional lattice configuration [7] in contrast to a simple linear chain in the single junction.

In general, there is a resonant phenomena between the Josephson plasma and the vortices in Josephson junction systems. It has known in the single Josephson junction that when the speed of the driven vortices matches with the propagation velocity of the Josephson plasma wave the resonance between them occurs and the emis-

*CREST, Japan Science and Technology Corporation (JST) Japan

sion power of the electromagnetic wave becomes a maximum [5]. Therefore, it has been the most important phenomenon from a point of view of electromagnetic wave emission and has been intensively investigated theoretically and experimentally not only the conventional single junctions but also intrinsic Josephson junctions. As a result, the existence of some resonant behaviors [8] and the important phenomena, that is, the superradiant state [9], [10] in which collective vortex motion resonates with the highest plasma mode and most of stacked junctions simultaneously synchronize have been found in intrinsic Josephson junctions. Especially, direct numerical simulation by one of authors(M.M) clearly revealed that the superradiant state might appear over an accessible wide range of I-V characteristics [10]. In this paper, we show the numerical results on those resonant flux flow states and review how the electromagnetic emission occurs related with those resonant states.

II. MODEL EQUATION AND JOSEPHSON PLASMA MODES

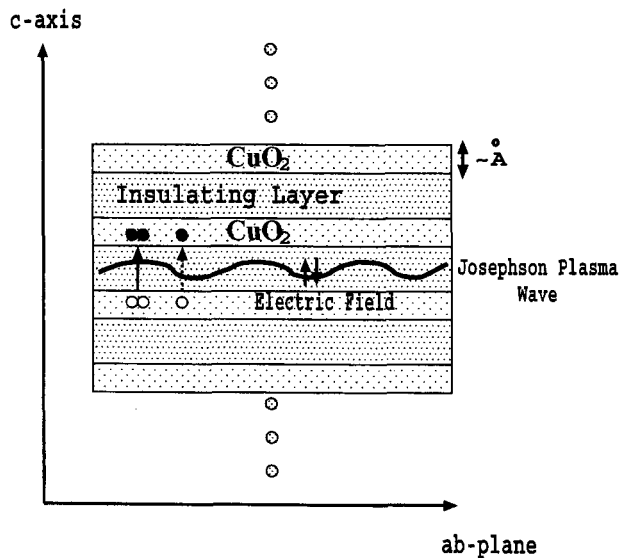


FIG.1 A schematic view of layered cuprates. Cooper pairs and quasi-particles tunnel between neighboring (double) CuO_2 layers. Those tunnel currents couple with electromagnetic field inside the insulating layer and form the Josephson plasma wave as an elementary excitation.

In layered High- T_c superconductors, a model in which the superconducting CuO_2 layers are electronically linked by the Josephson coupling through block layers has been confirmed by many experiments [1], [2]. Figure 1 shows a schematic view of the layered cuprate superconductors. When the phase difference between neighboring CuO_2

layers exists, the Josephson current flows along the c -axis and couples with the electromagnetic field inside dielectric layers. Since the phase difference is of a wave like, we call the wave Josephson plasma. An oscillating Josephson current always flows parallel to the c -axis, and therefore, the Josephson plasma waves can be classified into the longitudinal(propagation along the c -axis) and the transverse plasma(propagation along the ab -plane) waves respectively, depending on the directions of the wave propagation. Now, let us show the formulation for describing those plasma waves. The total current flowing along the c axis between ℓ -th and $\ell + 1$ -th double layers is given by

$$j_{\ell+1,\ell} = j_c \sin \varphi_{\ell+1,\ell} + \sigma_c E_{\ell+1,\ell} + \frac{\epsilon_c}{c} \frac{\partial E_{\ell+1,\ell}}{\partial t} \quad (1)$$

where σ_c and ϵ_c is the quasi-particle conductivity and the dielectric constant along the c -axis in the insulating layer, respectively. In Eq.(1) $\varphi_{\ell+1,\ell} (\equiv \theta_{\ell+1} - \theta_\ell - \frac{2\pi}{\phi_0} \int_\ell^{\ell+1} dz A_z)$ is the gauge invariant phase difference between the ℓ -th and $\ell+1$ -th layers, θ_ℓ being the phase at the ℓ -th layer, ϕ_0 the unit flux, and A_z the z component of the vector potential. The right hand side of Eq.(1) shows that the first term is the Josephson current, the second term the quasiparticle current, and the third term the displacement current. We notify that it is necessary to care the charge dynamics since the superconducting layer is atomic-scale and comparable to the charge screening length ($\sim \text{\AA}$) in layered cuprates as shown in Fig.1. In such a situation, the charge screening inside only a superconducting layer becomes not enough and the charge neutrality is dynamically broken [11] inside each superconducting layer by the electron tunneling as shown in Fig.1. In order to take account of this effect, we introduce the charge density ρ_ℓ in the ℓ -th superconducting layer expressed as

$$\rho_\ell = -\frac{1}{4\pi\mu^2} \left(\frac{\phi_0}{2\pi c} \frac{\partial \theta_\ell}{\partial t} + A_\ell^0 \right), \quad (2)$$

where μ is the Debye screening length and A_ℓ^0 is the scalar potential in the ℓ -th superconducting layer. Next, we derive basic model equations for the phase difference and the charge density. Here, for simplicity, we confine ourselves to x - z two dimension space, where x is one of the ab -plane direction and z the c -axis direction as shown in Fig.1. Inserting both the current (Eq.(1)) and the charge density (Eq.(2)) into the Maxwell equations and using the Josephson relations, we obtain the general coupled equations for both the phase difference and the charge density [12],

$$\begin{aligned} \frac{\partial^2 \varphi_{\ell+1,\ell}}{\partial t'^2} &= \frac{\partial^2 \varphi_{\ell+1,\ell}}{\partial x'^2} + \frac{1}{D\lambda_c} (\lambda_{ab}^2 - \epsilon_c \mu^2) \left(\frac{\partial \rho'_{\ell+1}}{\partial t'} - \frac{\partial \rho'_\ell}{\partial t'} \right) \\ &+ \frac{\lambda_{ab}^2}{sD} \Delta^{(2)} [\sin \varphi_{\ell+1,\ell} + \beta \frac{\partial \varphi_{\ell+1,\ell}}{\partial t'} + \beta \frac{\epsilon_c \mu^2}{D\lambda_c} (\rho'_{\ell+1} - \rho'_\ell)] \end{aligned}$$

$$-[\sin\varphi_{\ell+1,\ell} + \beta \frac{\partial\varphi_{\ell+1,\ell}}{\partial t'} + \beta \frac{\epsilon_c \mu^2}{D\lambda_c} (\rho'_{\ell+1} - \rho'_\ell)] \quad (3),$$

$$\left(\frac{\partial\varphi_{\ell+1,\ell}}{\partial t'} - \frac{\partial\varphi_{\ell,\ell-1}}{\partial t'} \right) + \frac{\epsilon_c \mu^2}{\lambda_c D} \Delta^{(2)} \rho'_\ell = \frac{s}{\lambda_c} \rho'_\ell \quad (4)$$

where $s(D)$ is the thickness of the superconducting (insulating) layers, $\lambda_{ab}(\lambda_c)$ is the penetration depth in the ab-plane (c-axis), $\beta \equiv \frac{4\pi\sigma_c\lambda_c}{\sqrt{\epsilon_c c}}$ is related with McCumber parameter β_c as $\beta_c \equiv 1/\beta^2$, and the operator $\Delta^{(2)}$ stands for a second difference defined as $\Delta^{(2)}f_{\ell+1,\ell} \equiv f_{\ell+2,\ell+1} + f_{\ell,\ell-1} - 2f_{\ell+1,\ell}$. In both equations time t , coordinate x , and the charge density ρ_ℓ are, respectively, normalized with $\frac{1}{\omega_p}$, λ_c , and $\frac{j_c}{\lambda_c \omega_p}$ where $\omega_p (\equiv \frac{c}{\sqrt{\epsilon_c \lambda_c}})$, λ_c , and j_c are the plasma frequency, the penetration depth along the c axis, and the c-axis critical current density, respectively. Basically, those equations can describe intrinsic Josephson effects in layered cuprates, however two more simplified equations have been so far employed due to their simple forms. The first one is a model equation derived by Koyama and Tachiki [6] and is applicable only for the longitudinal dynamics of the superconducting phase (It can be derived under a condition as $\lambda_{ab} \rightarrow 0$ in Eq.(3) and (4)). This is valid enough only when the phase difference is homogenous along ab-plane and the condition is considered to be realized in cases under no applied magnetic field. We note that the model can reproduce multiple-branch structures commonly seen in I-V characteristics along the c-axis in layered cuprate single crystals and can describe the dynamics of the longitudinal plasma [11]. The another one is called ‘‘coupled Sine-Gordon(CSG) equation’’ [13], [14] and is derived from Eq.(3) and (4) when the dynamical charge neutrality breaking effects are dropped ($\mu \rightarrow 0$ in Eq.(3) and (4)). This condition is valid enough for cases under the presence of the layer parallel magnetic field ($\lambda_{ab} \gg \mu$). Thus, the CSG equation has been regarded as the most basic equation which can describe dynamics of both the Josephson vortex and the plasma wave. In the rest of paper, we deal with only the CSG equation to concentrate on vortex dynamics and related plasma excitation. Now, let us return to the general equations Eq.(3) and (4), again. For obtaining the solution of the Josephson plasma, we make a liner approximation for Eqs. (3) and (4), since the amplitude of the phase is small. By solving the equation we obtain the frequency dispersions for the transverse and longitudinal plasmas are, respectively, obtained as

$$\omega_p^L(k_z) = \omega_p \sqrt{1 + \frac{\epsilon_c \mu^2}{sD} k_z^2 (s + D)^2}, \quad (5)$$

$$\omega_p^T(k_x) = \omega_p \sqrt{1 + \lambda_c^2 k_x^2} \quad (6).$$

Those dispersion relations are schematically shown in Fig.2. We note that the dispersion of the transverse plasma is much stronger than that of the longitudinal

plasma. This difference comes from the fact that the transverse plasma is a composite wave of the Josephson current and the electromagnetic field and asymptotic to that of the electromagnetic wave inside the junction insulating medium while the longitudinal plasma is a coupled wave of the Cooper pair density and only the electric field. Experimentally, the transverse plasma has first observed by Tamasuku et al. by measuring the plasma edge in reflectivity measurements of $\text{La}_{2-x}\text{Sr}_x\text{CuO}_4$ [15]. The longitudinal plasma has first measured by Matsuda et al. by measuring a sharp absorption peak in microwave measurements of Bi-2212 [16]. Although we confine ourselves two special modes propagating along the c-axis direction and the ab-plane, the Josephson plasma wave can propagate in any direction as shown in upper panel of Fig. 2. Then, the waves generally become mixtures of the transverse and longitudinal waves and their dispersions appear in the region shown by the hatch in Fig 2.

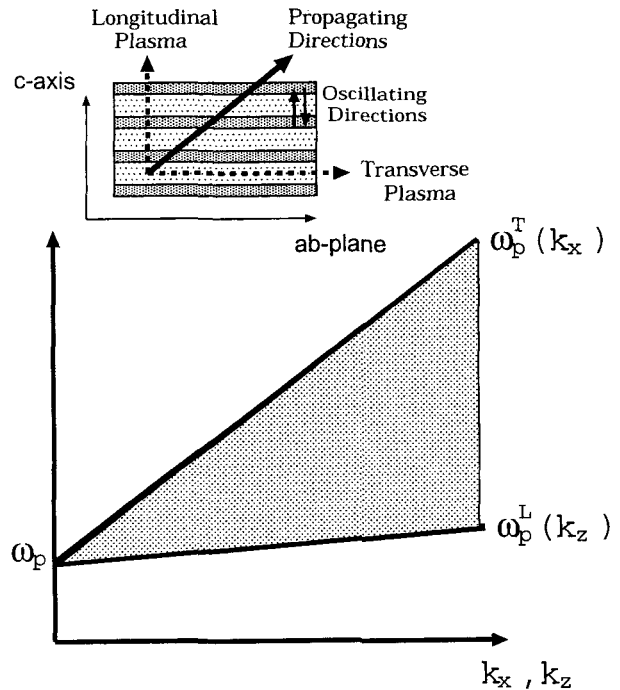


FIG.2 A schematic view of dispersion relations for longitudinal $\omega_p^L(k_z)$ and transverse plasma modes $\omega_p^T(k_x)$. Upper panel: the longitudinal mode propagates along the c-axis while the transverse one does parallel to ab-plane. When the propagating direction is inclined from those two special directions (dashed arrows) its dispersion lies in the hatched region depending on the propagating direction.

Next, let us consider about Josephson plasma modes in finite systems since the Josephson plasma modes described above are ones for infinite system. In fact, real samples in which many experiments in terms of vortex

dynamics are performed are composed of finite stacks of junctions, and therefore, the number of modes excited inside the sample are limited within finite number. Here, for simplicity, we give the dispersion relation of the excited plasma in a finite system by using the following CSG equation [14] expressed as

$$\begin{aligned} \frac{\partial^2 \varphi_{\ell+1,\ell}}{\partial t'^2} &= \frac{\partial^2 \varphi_{\ell+1,\ell}}{\partial x'^2} - \sin \varphi_{\ell+1,\ell} - \beta \frac{\partial \varphi_{\ell+1,\ell}}{\partial t'} \\ &+ \frac{\lambda_{ab}^2}{sD} \left(\frac{\partial^2 \varphi_{\ell+2,\ell+1}}{\partial t'^2} + \frac{\partial^2 \varphi_{\ell,\ell-1}}{\partial t'^2} - 2 \frac{\partial^2 \varphi_{\ell+1,\ell}}{\partial t'^2} \right) \\ &+ \frac{\lambda_{ab}^2}{sD} (\sin \varphi_{\ell+2,\ell+1} + \sin \varphi_{\ell,\ell-1} - 2 \sin \varphi_{\ell+1,\ell}) \\ &+ \beta \frac{\lambda_{ab}^2}{sD} \left(\frac{\partial \varphi_{\ell+2,\ell+1}}{\partial t'} + \frac{\partial \varphi_{\ell,\ell-1}}{\partial t'} - 2 \frac{\partial \varphi_{\ell+1,\ell}}{\partial t'} \right) \quad (7). \end{aligned}$$

This equation gives the following dispersion relation for a stack system composed of N junctions,

$$\omega^n(k_x) = \omega_p \sqrt{1 + \frac{\lambda_c^2 k_x^2}{1 + \frac{2\lambda_{ab}^2}{sD} (1 - \cos(\frac{\pi n}{N+1}))}}, \quad (8)$$

where N is the number of stacked junctions and n means the n -th mode among the modes ranged from 1 to N . Here, it should be noted that the dispersion relation is derived from a boundary condition in which $\varphi_{\ell+1,\ell}$ in 0-th and $N+1$ -th junction sites is set to be zero in Eq.(7) due to no presence of the junction at those sites. In such a condition, the c -axis propagating components form the standing waves along c -axis, and therefore, only the difference between modes is distinguished by their c -axis standing wave profiles as schematically depicted in the upper panel of Fig.3. The dispersions of those modes can be schematically illustrated inside the hatched region in the Fig.3, where the longitudinal plasma and the transverse plasma modes are also given for a comparison. In the dispersion relations it is found that the $n = 1$ mode gives the most dispersive relation while the $n = N$ mode is almost close to that of the longitudinal plasma. The $n = 1$ mode has no node inside junction as seen in the left hand side of upper pannel of Fig.3, while $n = N$ mode has $N-1$ nodes. Therefore, the excitation of the $n = 1$ mode is the most important point. If the Josephson vortices resonate with the mode, then the Josephson vortices are considered to form a almost rectangular lattice shape.

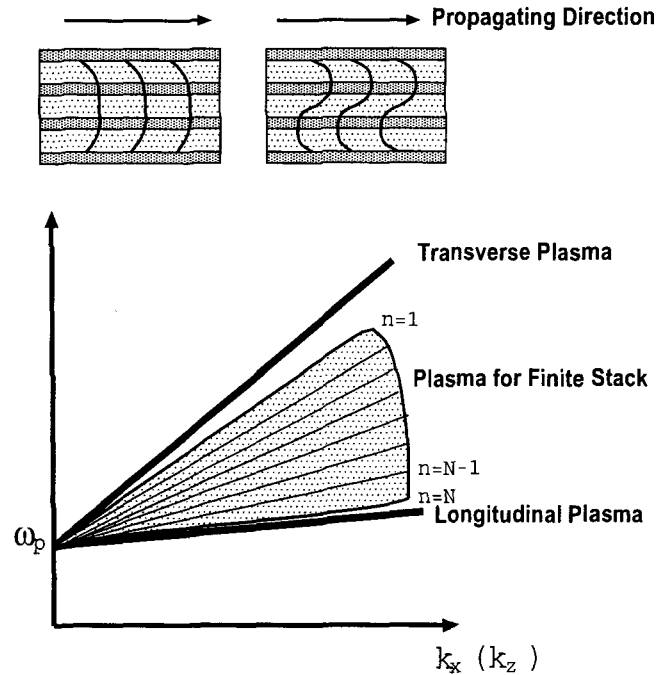


FIG.3 A schematic view of dispersion relations for the Josephson plasma standing wave modes in finite stack system $\omega^{(n)}(k_x) (n = 1 \sim N)$. Those dispersions are located inside the hatched region. The most dispersive mode is $n = 1$ -th mode while the most flat one is $n = N$ -th one. The dispersion relations of the longitudinal and the transverse mode are also depicted for a comparison.

III. INTERACTION BETWEEN VORTICES AND JOSEPHSON PLASMA

On an external magnetic field parallel to the ab -plane, the field penetrates into the sample in a form of Josephson vortex. The Josephson vortex is a non-linear solution of a set of Eqs. (3) and (4) and the CSG equation. Since the center of the vortex is situated in the block layer, the vortex has no normal core, instead only a current core. The magnetic field of the Josephson vortex extends over λ_{ab} from the vortex center along the c -axis and over λ_c along the a - b plane. Since λ_c is much longer than λ_{ab} , the magnetic field distribution has a shape of very flat ellipsoid extending in the direction of the a - b plane [4]. The Josephson vortices have no normal core and thus the pinning force and the friction force acting on the vortices are very weak [4]. When the vortices are driven by an external current flowing along the c axis, its speed attains up to 10^6 m/sec. The vortices moving with such a high speed strongly interact with the propagating plasma modes [1], [10], [17]. Moreover, since there are many modes propagating with different speeds depending on the c -axis profiles of the standing waves in finite

intrinsic Josephson junction systems, they have some resonant points and therefore, take various kinds of vortex lattice configurations according to the intensities of applied current and magnetic field [10], [17]. To investigate this phenomenon, we numerically solve the CSG Eq.(7).

A. Numerical Simulations of the Coupled Sine-Gordon Equation

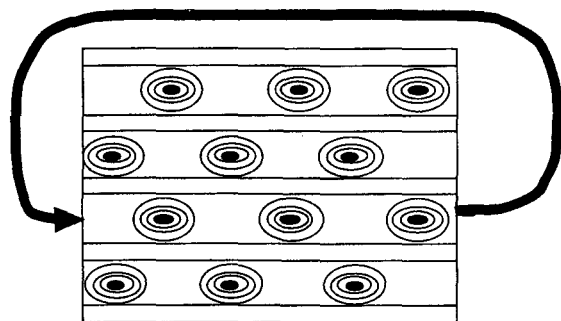


FIG.3 A schematic view for undertaking simulations. The periodic boundary condition is employed along the *ab*-plane direction.

Since both the Josephson plasma waves and the Josephson vortices can be described by the Eq.(7), the equation show that the moving vortices strongly interact with the Josephson plasma when the both move with a same speed [17]. This means that the moving vortices excite the Josephson plasma and consequently lead to an emission of electromagnetic wave. In numerical simulations of Eq.(7), we employ the periodic condition in the *a-b* plane direction as seen in Fig.3. This is because we wish to eliminate finite system size effects along the *a-b* plane in order to study fundamental resonant behavior between the Josephson plasma and the Josephson vortices. However, it should be noted that the open boundary condition is imposed along the *c*-axis and the excited plasma waves form the standing wave along the *c*-axis (See Eq.(8)). The computer simulations are performed in a two dimensional rectangular shape in which the size in the *ab*-plane are taken 10 mm and 40 junctions along the *c*-axis are stacked. This corresponds to a typical sample size in which the Josephson vortex dynamics are experimentally investigated. For the boundary condition for the surface of the top and bottom of

the sample, an external current is uniformly flow in and out, respectively. Now, let us show the simulation results. The typical simulation result for the current-voltage (*I-V*) characteristics is shown in Fig.4(I) in which some step like structures representing the existence of the resonance can be found. The typical snapshots of the flux flow states are shown in Fig.4 (a), (b), and (c). The horizontal lines in Fig.4(I) stand for the current values in which those snapshots are taken, while the vertical lines represent resonant points between moving vortices and the plasma waves estimated from taking $k_x = H_a$ (the applied field) in Eq.(8) [18]. From those figures it is found that the vortices form a conventional triangular lattice for a low voltage region before the first step structure appears in the *I-V* characteristics. When the current is increased from the triangular lattice flow state, the flow vortex configurations are changed as seen in Figs. 4(b) and 4(c). Those changes come from resonant phenomena between vortices and some different Josephson plasma [8], [10], [17]. We notify that the transitions between those different flow patterns are found to occur at the step like structures in the *I-V* characteristics by monitoring the vortex flow configurations. Among those many patterns we especially notify that an almost complete rectangular flow configuration like Fig.4(c) is stable between the two resonant voltage A and B in Fig. 4(I) and the region between them is relatively wider than other regions [10]. This is because resonant points as seen in Fig.4(I) are relatively sparse in the region between the points A and B. In this state the wave length and propagating velocity of the excited plasma wave are equal to the distance between the neighboring vortex in the same junction and the vortex velocity, respectively. This kind of the resonant state is called a superradiant state because the dynamics of the superconducting phase difference are coherent in almost all junctions and strong emissions are expected. In other words, that is a state that the highest plasma having no node along the *c*-axis is excited by the vortex motion. When a composite wave composed of the vortices and the plasma excited in this way goes out of the sample, a part of the wave is simply converted into the electromagnetic wave. Theoretical estimations for Bi-2212 predict that the power excited inside junction sites can reach up to order of 100mW/cm² [17] and the frequency range is in a Tera-Hertz region [10]. If the excited wave is efficiently converted into external electromagnetic wave, the intrinsic Josephson junction will be a quite useful Tera-Hertz wave generator. Experimentalists are now making various kinds of experiments for confirming this prediction.

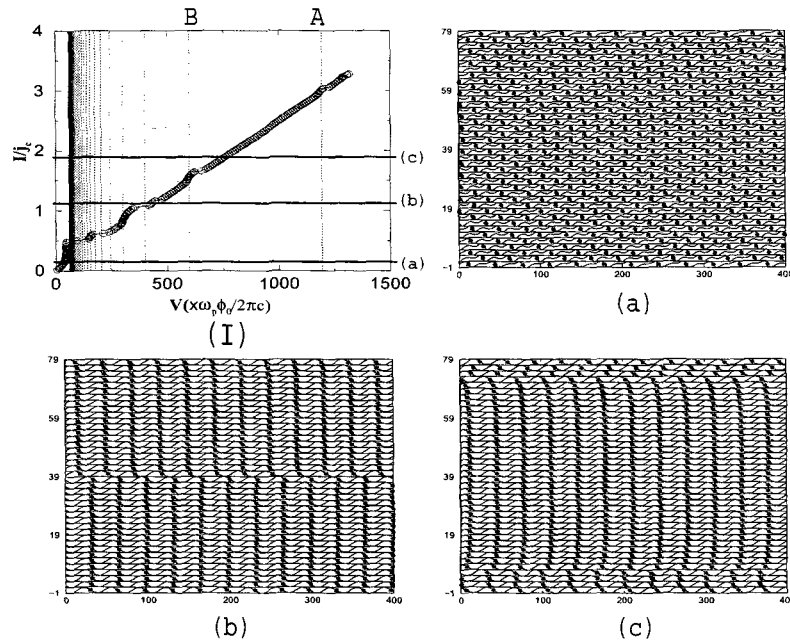


FIG.4 (I) The I-V characteristics. The vertical lines are resonant voltages estimated from the dispersion relation Eq.(8) and the horizontal lines mean the current values in which the following snapshots (a) (b) and (c) are measured. The modes assigned as A and B correspond to $n = 1$ and $n = 2$ modes in the dispersion relation, respectively. (a), (b), and (c) A snapshot of vortex centers and $\sin\phi$ in each junction site.

IV. SUMMARY AND CONCLUSION

In this paper we theoretically show that Josephson vortices driven by the transport current can exhibit the superradiance by finding numerically that the rectangular vortex lattice flow state essential for the superradiance is stable in a wide range of the I-V characteristics. Furthermore, by changing the transport current and the applied magnetic field, the frequency can be almost freely tuned over a wide range. Especially, under the high magnetic field ($\approx T_c$) we found that the frequency reaches to a THz range. In the future, we believe that if the superradiance is experimentally confirmed in intrinsic Josephson junctions, it should be one of the most important device applications in HTSC's materials.

- [3] M.Tachiki, T.Koyama, and S.Takahashi, *Phys.Rev.***B50**,7065,(1994).
- [4] J.R.Clem and M.W.Coffey, *Phys. Rev.* **B42**, 6209(1990).
- [5] A.Barone and G.Paterno, "Physics and Application of the Josephson Effect"(Wiley, New York, 1982).
- [6] T.Koyama and M.Tachiki, *Phys.Rev.***B54**,16183(1996).
- [7] L. Bulaevskii and J. R. Clem, *Phys.Rev.***B44**, 10234(1991).
- [8] R.Kleiner, *Phys.Rev.***B50**, 6919(1994).
- [9] A.V.Ustinov and S.Sakai, *Appl.Phys.Lett.* **73**,686(1998).
- [10] M.Machida, et al. *Physica C* **330**,85(2000).
- [11] M.Machida, T.Koyama, and M.Tachiki, *Phys.Rev.Lett.***84**,4618(1999).
- [12] M.Machida et al. *Physica C* **331**,85(2000).
- [13] S.Sakai et al, *J.Appl.Phys.***73**(5), 2411(1993).
- [14] L.N.Bulaevskii et al.,*Phys.Rev.***B50**,12831(1994).
- [15] K.Tamasaku et al.,*Phys.Rev.Lett.***69**,1455(1992).
- [16] Y.Matsuda et al.,*Phys.Rev.Lett.***75**,4512(1995).
- [17] A. E. Koshelev and I. S. Aranson, *Phys. Rev. Lett.***85**, 3938(2000).
- [18] Since the wave number of the excited wave along the ab-plane is affected by the periodicity of the Josephson vortices, A matching condition as $k_x = H_a$ is employed

[1] R.Kleiner et al.,*Phys.Rev.Lett.***68**,2394(1992).

[2] G.Oya, et al.,*Jpn.J.Appl.Phys.***31**,L829(1992).

(Received March 19 8, 2001; Accepted April 9, 2001)